Analysis and Modelling of Liquid Phase Turbulence Kinetic Energy Equation in Bubbly Flows via Direct Numerical Simulation

Sercan Erdogan, Martin Wörner

Karlsruhe Institute of Technology (KIT), Institute of Catalysis Research and Technology
P.O. Box 3640, 76021 Karlsruhe, Germany

ABSTRACT

We perform direct numerical simulations (DNS) of bubble swarms in a sub-region of a flat bubble column by a volume-of-fluid method. The flow is buoyancy-driven and the overall void fraction is about $2\ \%$. The Morton number is in the range $2.2\times10^{-8} \le M \le 3.1\times10^{-7}$ while the range of the Eötvös number is $0.747 \le Eö_{\mathrm{B}} \le 2.625$. We use the DNS data to evaluate the terms in the analytical transport equation of the liquid phase turbulence kinetic energy. For the case of pseudo-turbulence considered here, the interfacial term constitutes the main source term in this equation. We test literature models for closure of the interfacial term against the DNS data. None of the tested models performs well for all cases and model improvements are required.

Keywords: Bubble induced turbulence, DNS, Statistical turbulence models, Bubble column

1. Introduction

Experience, empirical correlations, one-dimensional convection-dispersion models and compartment models form usually the basis for the design of industrial scale bubble columns. Such approaches remain somewhat limited when one aims on the increase of the reactor performance. Multidimensional CFD methods are potentially attractive for this purpose, however, not yet used as tool for design of industrial scale bubble columns.

Several papers in literature investigated the suitability and limitations of different modeling concepts for bubble columns (see e.g. [1] for a concise overview). Though the conclusions are not definite, several authors report that predictions of the mean flow (mean velocities, mean gas-hold-up) and the turbulent kinetic energy obtained by using the k–ε models are comparable to those obtained by using Reynolds-stress models or Large-eddy simulations [2-5]. However, all model approaches have deficiencies concerning turbulent quantities, which often do not compare well with experiments. This deficit is of special importance for population balance approaches where turbulence data enter in breakup and coalescence kernels. Therefore, improved closure relations for k and ε are necessary for bubble-driven flows.

In bubble columns, the rising bubbles create an unsteady buoyancy-driven flow and induce large recirculation loops in the liquid phase. This generates shear-induced turbulence (especially near the walls) and bubble-induced turbulence (BIT or pseudo-turbulence). Neither pure pseudo-turbulence is fully understood nor its inherent non-linear interaction with shear-induced turbulence. For reliable mathematical modeling of pseudo-turbulence in bubbly flows, it is essential to understand the underlying physics. For detailed discussions on physics of pseudo-turbulence, and also on CFD methods for bubble columns and turbulence closures in k–ε type models as well as the k_{L} equation we refer to [1].

Kataoka & Serizawa [6] derived the exact equations for k and ε for a gas-liquid flow consisting of two incompressible phases. In the exact k_{L} equation, all terms involving fluctuating quantities must be modeled to close the system of equations. Experimentally, it is difficult to obtain data about the terms in the k_{L} equation especially under non-dilute conditions. However, direct numerical simulations (DNS) on sufficiently fine grids can provide such data.

Ilić [7] performed DNS studies of laminar bubbly flow in a narrow vertical channel in rather viscous liquids (Morton number $M > 3\times10^{-6}$) and evaluated all terms in the k_L equation for a single bubble [8] and a swarm consisting of up to eight bubbles [9]. For all closure terms, she compared the DNS profiles with model predictions. Ilić found that for the production by shear stresses all models yield a strong overestimation, while for the turbulent diffusion all models used in engineering codes result in an underestimation. For the interfacial term, Ilić analyzed a number of models and identified a promising one. However, all the other closure terms in the kinetic energy equation need further improvement for bubbly flows [7].

In this paper we extend the DNS study of Ilić [7] on BIT in mono-disperse bubble swarms on lower values of the Morton number and also investigate the influence of the Eötvös number and gas hold-up on the k_L equation and closure relations for the interfacial term.

2. Numerical simulations

The DNS computations are performed with the in-house computer code, TURBIT-VOF which uses a volume-of-fluid method with piecewise linear interface reconstruction for describing the interface evolution. For details on the governing equations and the numerical method we refer to [10].

2.1. Numerical set-up

We consider a cubic computational domain, which represents a sub-region of a flat bubble column. In vertical (x) and span-wise (y) direction, we specify periodic boundary conditions whereas in z-direction the domain is bounded by two vertical sidewalls (distance L_{wall}) with no-slip condition. The simulation conditions are set so, that in the center of the planar channel the bubbles rise due to buoyancy, whereas near the sidewalls a downward liquid flow occurs.

TURBIT-VOF uses a Cartesian grid, which is equidistant in x- and y-direction and optionally equidistant or not in z-direction. By a non-equidistant grid, it is easier to ensure that the liquid film between the bubble and the wall is well resolved. Due to the downward liquid flow near the sidewalls, the lift force acts away from the wall; this avoids an unwanted contact of bubbles with the walls during the simulation.

2.2. Preliminary parametric studies

We performed a number of test runs for single bubbles in order to identify parameters, which allow efficient simulations without comprising the physics. We found that a grid resolution of 20 mesh cells per bubble diameter and a liquid-to-gas density ratio of 25 are sufficient to obtain results that are independent on both, the mesh size and the gas density, ρ_G. This density ratio is also typical for real systems under high pressures.

Beside the influence of the gas-liquid density ratio, we also studied the effect of the gas-liquid viscosity ratio $\Gamma_\mu = \mu_G/\mu_L$, which we varied in the range $0.1 \le \Gamma_\mu \le 1$. When the liquid viscosity and all other parameters are fixed, Γ_μ has no significant effect on the bubble rise velocity. However, it has influence on the velocity profiles in the wake and the intensity of the recirculation in the bubble. This effect is especially noticeable between the cases with $\Gamma_\mu = 1$ and $\Gamma_\mu = 0.5$ while the difference between cases with $\Gamma_\mu \le 0.5$ is very small. For very low viscosity ratio, a small time step width is required which drastically increases required CPU time to reach quasi-steady state condition. In the present simulations, therefore, the viscosity ratio $\Gamma_\mu = 1/3$ and $\Gamma_\mu = 1$ is used.

2.3. Bubble swarm simulations

We performed numerical simulations for bubble swarms for two scenarios, where we vary some parameters while others are fixed, see **Table 1** and **Table 2**. The values of the liquid density slightly differ for Scenario A and B while the liquid-to-gas density ratio is always $\rho_G/\rho_L = 1/25$. The liquid viscosity is in the range $0.44\ \text{mPas} \le \mu_L \le 5\ \text{mPas}$. The surface tension is in the range $0.0028\ \text{N/m} \le \sigma \le 0.028\ \text{N/m}$. These variations yield values of the Morton number in the range $2.2\times10^{-8} \le M \le 3.1\times10^{-7}$. The volume equivalent bubble diameter is in the range $1\ \text{mm} \le d_B \le 3\ \text{mm}$ which corresponds to Eötvös numbers in the range $0.747 \le Eö_B \le 2.625$. The cases with $M \approx 10^{-7}$ are started from spherical bubbles with both, liquid and gas at rest. Instead, the cases for $M \approx 10^{-8}$ are started from simulations runs with $M \approx 10^{-7}$. For most cases, the simulations have already achieved statistically steady flow conditions while some cases are still running.

A critical issue in the bubble swarm simulations is the overall void fraction. Here, we are interested in mono-disperse flows. Bubble coalescence is therefore unwanted. In DNS of interfacial flows, coalescence is an unresolved problem as it often either occurs artificially or is suppressed at all [11]. In our VOF method coalescence is initiated when the distance between two bubbles is less than the size of a mesh cell [1] and is therefore grid-dependent. To avoid coalescence, we consider low void fractions here. From many tests, we found that a holdup ε of about $2.5\ \%$ is a reasonable upper limit for preserving mono-disperse flow in our simulations. Occasionally, coalescence occurs even for lower values of ε. In the present set-up, ε depends on the ratio d_B/L_{wall} and on the number of bubbles within the cubic domain. Here, we choose $L_{wall} = L_{ref} = 5\ d_B$. The number of bubbles within the computational domain is either five or six. This corresponds to an overall gas content of $\varepsilon = 2.1\%$ and $2.5\ \%$, respectively.

From the mean velocity of bubbles in the swarm we computed a mean value of the bubble Reynolds number, Re_B, which is in the range $35 - 230$. As expected, Re_B increases for scenario A with increase of d_B and $Eö_B$ and increases for scenario B with decrease of the Morton number.

Table 1: Scenario A - Cases with variation of $Eö_B$ and ε and following fixed parameters: $\rho_L = 867$ kg/m^3, $\sigma = 0.028$ N/m, $\mu_L = 5$ mPas, $M = 3.1\times10^{-7}$, $\mu_G/\mu_L = 1/3$. Non-equidistant grid with 100×100×120 cells.

Case	A1	A2	A3	A4
Bubbles	5	5	5	6
ε [%]	2.1	2.1	2.1	2.5
d_B [mm]	1.6	2.0	3.0	2.0
$Eö_B$	0.747	1.167	2.625	1.167
Re_B (mean)	35	55	115	60

Table 2: Scenario B - Cases with variation of the Morton number and following fixed parameters: 6 bubbles, $\rho_L = 752$ kg/m^3, $\varepsilon = 2.5\%$, $d_B = 1$ mm, $\sigma = 0.0028$ N/m, $Eö_B = 2.53$, $\mu_G/\mu_L = 1$. Equidistant grid with 100×100×100 cells.

Case	B-M7	B-M8
μ_L [mPas]	0.79	0.44
M	2.2×10^{-7}	2.2×10^{-8}
Re_B (mean)	125	230

2.4. Statistical analysis of DNS results

Analysis of the k_L equation requires the appropriate averaging of the instantaneous flow field within the computational domain. For the bubbly flow between vertical parallel plates, the vertical and span-wise directions can be considered as homogeneous, which allows the spatial averaging over vertical slabs of mesh cells parallel to the channel walls [7, 12]. This yields profiles of statistical quantities, which depend on the wall-normal coordinate z. In addition, we average the data over different instants in time within the statistically steady regime. We denote the respective plane and time averaging by a double overbar, i.e. it is

$$k_L = \frac{1}{2}\overline{\overline{\mathbf{u}_L'^2}} \tag{1}$$

3. Results and Discussion

3.1. Distribution of kinetic energy

In Fig 1 we show wall-normal profiles of the liquid turbulence kinetic energy for different cases. We see that for scenario A the magnitude and integral value of k_L increases with increase of d_B and $Eö_B$ while for scenario B it increases with the decrease of the liquid viscosity and Morton number. For each scenario, the liquid turbulent kinetic energy thus increases with increase of the bubble Reynolds number. However, a comparison of case B-M7 and case B-M8 with case A4 shows that in the former two cases k_L is lower though Re_B is higher. We attribute this to the different values of the viscosity ratio, which notably influences the liquid velocity in the bubble wake (see discussion above).

Between the cases A2 and A4 it is difficult to make a certain comparison in terms of void fraction since for case A4 coalescence occurs two times between different bubble couples thus eventually two initial size and two bubbles with double volume exist in the time interval of the statistical analysis. If we pay attention to the curve with blue circles (case A4), we can realize the influence of the different bubble sizes in the bi-disperse flow. The kinetic energy curve is not symmetrical since the main interfacial term is higher at certain regions depending on the higher void fraction of the merged bubbles. For other cases, almost symmetrical curves appear even though slight changes are visible. This is because the evaluation period in a statistically

steady state is not yet sufficient. Therefore, we continue these simulations to allow time averaging over larger intervals.

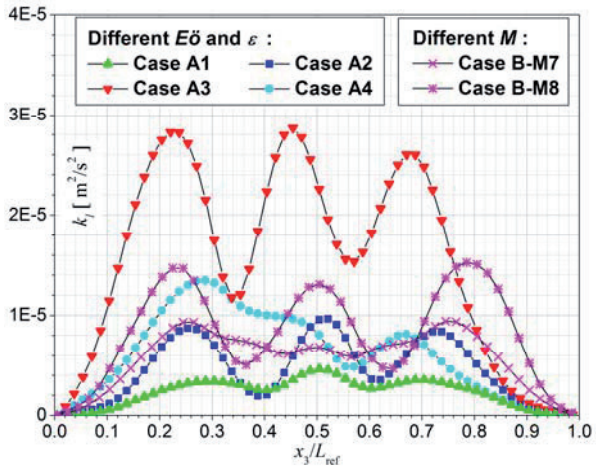

Fig 1 Kinetic energy of liquid velocity fluctuations generated by bubble rise through liquids.

3.2. Budget of exact k_L equation

In Fig 2, we present the wall normal profiles of different terms in the k_L equation as evaluated from the DNS data for case B-M7 (for a mathematical definition of these terms we refer to [7]). Also shown is the profile of the gas volume fraction. The interfacial term, Υ, contains the specific interfacial area a_i and is thus specific for two-phase flows. Comparing the profile of Υ with that of α_G shows that Υ has large positive values in regions with high void fraction and is zero in regions always occupied by liquid. This indicates that the rising bubbles create velocity fluctuations in the bubble wakes and thereby pseudo-turbulence. Clearly, Υ is the main source of liquid turbulence kinetic energy whereas production by shear stresses is negligible. The same result is reported in [7].

The magnitude of the dissipation rate of k_L is very large in two-phase regions but is non-zero in pure liquid regions close to the walls. Thus, production and dissipation are not in local equilibrium. Instead, molecular and turbulent diffusion redistribute the surplus of production in regions of high void fractions toward regions of low or zero void fraction. So to say, diffusion processes transport the energy generated by bubble interfaces from the two-phase regions towards the single-phase regions.

3.3. Interfacial turbulence transfer

Since the interfacial term Υ constitutes the main source of k_L, one should model this term properly. In literature, several models have been proposed for closure of this term, see e.g. [2]. Here, we compare the profile of the exact interfacial term in the k_L equation as evaluated from our DNS data with profiles predicted for Υ by different models.

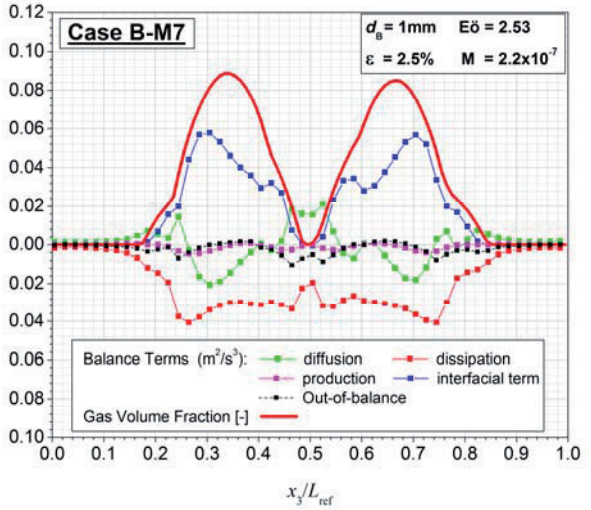

Fig 2 Budget of the exact k_L equation for Case B-M7 where $\Gamma_\mu = 1$.

Closure assumptions from literature relate the interfacial term in various ways to the rate of work performed by hydrodynamic forces. The most important hydrodynamic force is the drag force F_D. By taking the product of F_D with the relative velocity between the phases, we obtain the respective work as

$$W_D = F_D \left|\overline{\overline{\mathbf{u}_r}}\right| = \frac{3}{4} C_D \frac{\alpha_G \rho_L}{d_B} \left|\overline{\overline{\mathbf{u}_r}}\right|^3 \qquad (2)$$

Here, C_D is the drag coefficient. In **Table 3** we list the three different models from literature which we test here against the DNS data.

Table 3: Models for interfacial term Υ in k_L equation.

Reference	Model for interfacial term Υ	C_D
(LL) [13]	W_D	$\frac{2}{3}\sqrt{Eö_B}$
(OL) [14]	$0.75 W_D$	$\frac{2}{3}\sqrt{Eö_B}$
(PB) [15]	$1.44(1-\alpha_G) W_D$	0.44

In the model of Lopez & Lahey (LL) [13] the interfacial term is $\Upsilon = W_D$, while the models of Olmos et al. (OL) [14] and Pfleger & Becker (PB) [15] both include a prefactor. The drag coefficient in models LL and OL are evaluated from the Ishii & Zuber model [16] as C_D =

$(2/3)Eö_B^{0.5}$. For Eötvös numbers in the range $0.747 - 2.625$ we obtain from this correlation drag coefficients in the range $0.576 \leq C_D \leq 1.08$. The constant value $C_D = 0.44$ in the PB model is valid for flow around a rigid sphere at Reynolds number $Re_B > 1000$ while for our cases Re_B is much lower and in the range $35 - 230$.

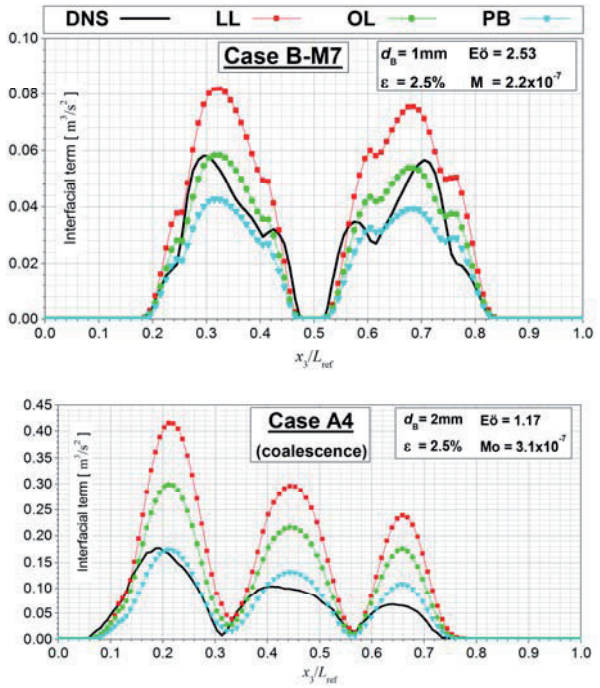

Fig 3 Predictions of interfacial turbulence transfer by engineering models for case B-M7 (top) and case A4 with coalescence (below).

In Fig 3, we test the performance of the three closure relations for different scenarios. For case B-M7 where $\Gamma_\mu = 1$ the closest approximation to the DNS curve is obtained by the model OL while PB and LL over- and underestimates it, respectively. For case B-M7 and case B-M8 (which is not shown here), we observed that the same models show similar behavior for the magnitude of the curves.

For case A4, where the coalescence occurs, the PB model gives an acceptable match with the magnitude of interfacial term curve while other models overestimate it. Besides, all the models reflect the bias caused by coalescence, although we use the initial d_B value for $Eö_B$ in C_D to calculate Υ, not the d_B value after coalescence. For models LL and OL, we evaluate C_D from $Eö_B$ for mono-disperse flow. If we insert $C_D = (2/3)Eö_B^{0.5}$ into Eq. (2), then d_B cancelles so that the influence of coalescence on Υ only occurs via the volumetric fraction α_G. Thus, models that define Υ proportional to W_D with $C_D = (2/3)\, Eö_B^{0.5}$ do not account at all for the influence of the bubble diameter and its change.

For the PB model this is not the case since C_D is constant, hence, the value of d_B in Eq. (2) is still in charge. If we consider the volume-equivalent diameter of two coalesced bubbles for calculation of F_D, due to inverse proportion the value of Υ would be 26% lower, which means a large under-estimation of Υ would occur at the location of the coalesced bubbles (at $x_3/L_{ref} \approx 0.2$).

The PB model provides the best fit for cases A2 and A3 as well. Therefore, we show only the results for the PB model in Fig 4 where we compare predictions for exactly same cases but only with different bubble diameter. Less interfacial area is present with smaller bubbles (case A2) and therefore they create less interfacial turbulence than bigger ones (case A3). For case A3, lateral motion of bubbles occurs by the increase of Re_B and therefore the interfacial term does not become zero in most part of the domain except near wall regions. Here, another point is notable: even for case A3, the model PB (also LL and OL, which we do not show here) partially reflects the alteration in the magnitude of the DNS curve.

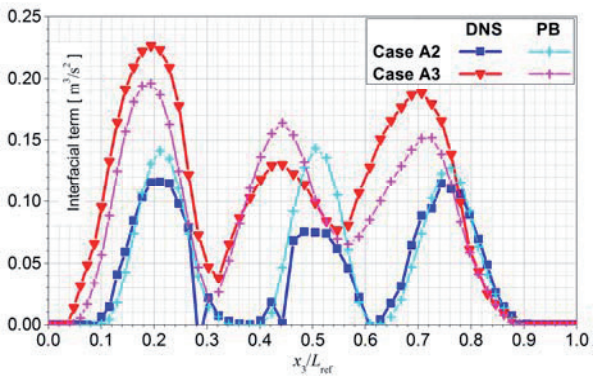

Fig 4 Comparison of PB model for interfacial term with DNS results for case A2 and case A3.

4. Conclusions

In this paper, we performed direct numerical simulations of bubble swarms in a sub-region of a flat bubble column with a volume-of-fluid method for void fractions of about 2 %. From the DNS data, we evaluated the liquid phase turbulent kinetic energy k_L and its analytical transport equation. The evaluation of the individual terms in the k_L equation showed that the main source term is due to the action of

interfaces while production by shear stresses is negligible. Production and dissipation are not in local equilibrium, and molecular and turbulent diffusion redistribute the surplus of production of k_L from regions of high to low void fractions.

In its modeled form, the k_L equations is a cornerstone for CFD simulations of bubbly flows with statistical turbulence models based on the Euler-Euler approach. Here, we used the DNS results for a priori-testing of closure assumptions for the interfacial term in the k_L equation. We find that the model of Pfleger and Becker [15] gives relatively good results for different cases even though it is strictly valid only for certain range of Re_B which doesn't match with our conditions. On the other hand the model of Olmos et al. [14] is a better approximation for the cases with $\Gamma_\mu = 1$. All the tested models reflect the changes of the system parameters (even for coalescence) on the magnitude of the curves qualitatively, but not quantitatively.

To allow for a better comparison between different models for the interfacial term, we will restrict the evaluation in future tests to a single drag relation. For that purpose, we will use the drag coefficient of Tomiyama et al. [17] which has been verified for a wide parameter range.

As next step, we will use the DNS data to develop improved models for the interfacial term and other closure terms (especially diffusion term) in the k_L equation. We will implement these in an Euler-Euler OpenFOAM solver and validate the models by experimental data for flows in bubble columns.

Acknowledgment

We gratefully acknowledge the support of the Federal Ministry of Education and Research for funding this project (BMBF FKZ 033RC1102H).

REFERENCES

1. Wörner, M. and S. Erdogan, Toward Improved Closure Relations for the Turbulent Kinetic Energy Equation in Bubble-Driven Flows. Chem Ing Techn, 2013. 85(7): p. 1131-1136.
2. Zhang, D., N.G. Deen, and J.A.M. Kuipers, Numerical simulation of the dynamic flow behavior in a bubble column: A study of closures for turbulence and interface forces. Chem Eng Sci, 2006. 61(23): p. 7593-7608.
3. Dhotre, M.T., B. Niceno, and B.L. Smith, Large eddy simulation of a bubble column using dynamic sub-grid scale model. Chem Eng J, 2008. 136(2-3): p. 337-348.
4. Tabib, M.V., S.A. Roy, and J.B. Joshi, CFD simulation of bubble column - An analysis of interphase forces and turbulence models. Chem Eng J, 2008. 139(3): p. 589-614.
5. Silva, M.K., M.A. d'Avila, and M. Mori, Study of the interfacial forces and turbulence models in a bubble column. Computers & Chemical Engineering, 2012. 44: p. 34-44.
6. Kataoka, I. and A. Serizawa, Basic Equations of Turbulence in Gas-Liquid 2-Phase Flow. Int J Multiphase Flow, 1989. 15(5): p. 843-855.
7. Ilic, M., Statistical analysis of liquid phase turbulence based on direct numerical simulations of bubbly flows 2006, Wissenschaftl. Berichte Forschungszentrum Karlsruhe FZKA 7199.
8. Ilic, M., M. Wörner, and D.G. Cacuci, Balance of liquid-phase turbulence kinetic energy equation for bubble-train flow. J Nucl Sci Techn, 2004. 41(3): p. 331-338.
9. Wörner, M., et al., Volume-of-fluid method based numerical simulations of gas-liquid two-phase flow in confined geometries. Houille Blanche, 2005(6): p. 91-104.
10. Öztaskin, M.C., M. Wörner, and H.S. Soyhan, Numerical investigation of the stability of bubble train flow in a square minichannel. Physics of Fluids, 2009. 21(4): p. 042108.
11. Wörner, M., Numerical modeling of multiphase flows in microfluidics and micro process engineering: a review of methods and applications. Microfluid Nanofluid, 2012. 12: p. 841-886.
12. Ilic, M., M. Wörner, and D.G. Cacuci, Investigations of liquid phase turbulence based on direct numerical simulations of bubbly flows, in NURETH-11. 2005: Avignon, France.
13. Lopez de Bertodano, M., R.T. Lahey, and O.C. Jones, Phase Distribution in Bubbly 2-Phase Flow in Vertical Ducts. Int J Multiphase Flow, 1994. 20(5): p. 805-818.
14. Olmos, E., C. Gentric, and N. Midoux, Numerical description of flow regime transitions in bubble column reactors by a multiple gas phase model. Chem Eng Sci, 2003. 58(10): p. 2113-2121.
15. Pfleger, D. and S. Becker, Modelling and simulation of the dynamic flow behaviour in a bubble column. Chem Eng Sci, 2001. 56(4): p. 1737-1747.
16. Ishii, M. and N. Zuber, Drag Coefficient and Relative Velocity in Bubbly, Droplet or Particulate Flows. AICHE Journal, 1979. 25(5): p. 843-855.
17. Tomiyama, A., et al., Drag coefficients of single bubbles under normal and micro gravity conditions. JSME Int. J. Series B-Fluids and Thermal Engineering, 1998. 41(2): p. 472-479.